FAR ULTRAVIOLET IMAGING FROM THE IMAGE SPACECRAFT: 2. WIDEBAND FUV IMAGING

S. B. MENDE, H. HEETDERKS, H. U. FREY, M. LAMPTON, S. P. GELLER, R. ABIAD,
O. H. W. SIEGMUND, A. S. TREMSIN,
Space Sciences Laboratory, University of California Berkeley, Berkeley, CA 94720
J. SPANN,
George C. Marshall Spaceflight Center, Huntsville AL 35812
H. DOUGANI
Tala Advanced Applications, Inc., Madison, AL 35758
S. A. FUSELIER, A. L. MAGONCELLI, M. B. BUMALA,
Lockheed Martin Advanced Technology Center, Palo Alto, CA, 94304
S. MURPHREE, T. TRONDSEN
University of Calgary, Calgary, Canada ABT2N 1N4

Abstract. The Far Ultraviolet Wideband Imaging Camera (WIC) complements the magnetospheric images taken by the IMAGE satellite instruments with simultaneous global maps of the terrestrial aurora. Thus, a primary requirement of WIC is to image the total intensity of the aurora in wavelength regions most representative of the auroral source and least contaminated by dayglow, have sufficient field of view to cover the entire polar region from spacecraft apogee and have resolution that is sufficient to resolve auroras on a scale of 1 to 2 latitude degrees. The instrument is sensitive in the spectral region from 140-190 nm. The WIC is mounted on the rotating IMAGE spacecraft viewing radially outward and has a field of view of 17° in the direction parallel to the spacecraft spin axis. Its field of view is 30° in the direction perpendicular to the spin axis, although only a 17° x 17° image of the Earth is recorded. The optics was an all-reflective, inverted Cassegrain Burch camera using concentric optics with a small convex primary and a large concave secondary mirror. The mirrors were coated by a special multi-layer coating, which has low reflectivity in the visible and near UV region. The detector consists of a MCP-intensified CCD. The MCP is curved to accommodate the focal surface of the concentric optics. The phosphor of the image intensifier is deposited on a concave fiberoptic window, which is then coupled to the CCD with a fiberoptic taper. The camera head operates in a fast frame transfer mode with the CCD being read approximately 30 full frames (512 by 256 pixel) per second with an exposure time of 0.033 s. The image motion due to the satellite spin is minimal during such a short exposure. Each image is electronically distortion corrected using the look up table scheme. An offset is added to each memory address that is proportional to the image shift due to satellite rotation, and the charge signal is digitally summed in memory. On orbit, approximately 300 frames will be added to produce one WIC image in memory. The advantage of the electronic motion compensation and distortion correction is that it is extremely flexible, permitting several kinds of corrections including motions parallel and perpendicular to the predicted axis of rotation. The instrument was calibrated by applying ultraviolet light through a vacuum monochromator and measuring the absolute responsivity of the instrument. To obtain the data for the distortion look up table, the camera was turned through various angles and the input angles corresponding to a pixel matrix were recorded. It was found that the spectral response peaked at 150 nm and fell off in either direction. The equivalent aperture of the camera, including mirror reflectivities and effective photocathode quantum efficiency, is about 0.04 cm^2. Thus, a 100 Rayleigh LBH aurora is expected to produce 23 equivalent counts per pixel per 10 s exposure at the peak of instrument response.

1. Introduction

In a companion paper (Paper 1) we have discussed the IMAGE auroral imaging requirements. In summary, the Wideband Imaging Camera (WIC) is required to image the total intensity of the aurora in wavelength regions most representative of the auroral source and least contaminated by dayglow and other undesirable sources. It must also have sufficient field of view to cover the entire polar region from spacecraft apogee, and have resolution that is sufficient to resolve auroras on a scale of 1 to 2 latitude degrees.

After almost three decades of auroral imaging from satellites, the advantages of this observational technique have become well established. With every technological improvement have come new scientific discoveries. Initially focusing on visible auroras, it quickly became apparent that much more extended coverage could be obtained by utilizing the ultraviolet portion of the spectrum. First successfully implemented by the Dynamics Explorer program,

DE-1 utilized a combination of filters and scanning mirrors to detect UV emissions (among others) in several broad bands (Frank et al., 1981). This mission also established the importance of multiple images per satellite orbit, thereby providing for the first time reasonable temporal information on the hemispheric auroral distribution.

Two technical improvements over the DE-1 system were realized by the Viking Imager program implemented by the Canadian Space Agency (Anger et al., 1987): Exposing all regions of an image at the same time (thereby reducing uncertainties in the timing of observations), and providing the ability to image from a spinning satellite. The introduction of area detectors, specifically, charge-coupled devices (CCD), allowed the design of an imager capable of imaging large areas of the Earth with every pixel within the image exposed at the same instant of time. Installed on a spinning satellite, images could be acquired at a repetition rate equal to the spin period by implementing a method to shift the charge at the spin rate of the satellite, thereby keeping the image from blurring.

In order to provide a suitable camera system for the restricted number of photons that would be imaged on a spinning satellite, it was necessary to employ a fast camera. The design chosen was an inverted Cassegrain Burch type camera, operating at f/1 (Burch, 1947). The camera was housed inside a graphite fiber epoxy composite (GFEC) tube, a material that was intended to provide the necessary thermal expansion characteristics over the expected operating temperature range. In the Canadian program, the instrument was designed to mount on a platform that exposes the instrument to space, and the expected operating temperature range of the instrument was much larger than the environment expected in the interior of the IMAGE spacecraft. The camera had a field of view of approximately 30° x 30° and was fitted with baffles to reduce scattered light by a factor of 2.5×10^{-4}.

Subsequent to the Viking program, the opportunity to make further improvements was provided by the Freja program (Murphree et. al., 1994). In this low altitude mission, the satellite spin rate was significantly higher, resulting in effective integration times of approximately 0.3 s. In addition, the satellite altitude required extending the field of view of the camera system beyond the nominal 30° in order to observe the entire Earth. This was accomplished by matching the CCD readout rate to the satellite spin rate so that data could be continuously read into memory, theoretically allowing images of a complete spin to be acquired.

The final utilization of this design was in the Russian Interball program (Cogger et al., 1995). In this program, two identical cameras were employed. But because of the orbital configuration, one was mounted at 67.5° to the spin axis, not at 90° as is normal. This was to take advantage of the changing orbit and to allow more complete coverage of the auroral distribution. This required more sophisticated tapers connecting the MCP to the CCD.

It was established (See Paper 1) that the IMAGE satellite needed a similar Wideband Imaging Camera (WIC) with a field of view of about 20°. This imager needed to operate in the far ultraviolet spectral range. Thus, the IMAGE requirements were very similar to those of the cameras used on the Viking/Freja satellite missions and, therefore, this camera design was adopted for the IMAGE mission.

Instruments on IMAGE view radially outward away from the spin axis. The spin axis is perpendicular to the orbit plane. The orbit is truly polar (90° orbital inclination) with apogee at 44,000 km and perigee at 1000 km. For the first two years of the mission, apogee is over the Northern Hemisphere and after one year after launch, directly above the pole. The satellite will spend most of its time far away from Earth, observing at and near apogee. The FUV auroral instruments view the Earth for a brief time– once per satellite revolution (period of revolution = 2 min.). During certain seasons the sun is near the satellite orbit or spin plane and therefore it is possible for it to illuminate the IMAGE FUV optical apertures. Sun sensors are included in the FUV package that protect the instruments by reducing the high voltage to a few hundred volts to minimize damage from the high solar UV fluxes. It should be mentioned that during times when it is possible to have a solar eclipse at the satellite, by either the Earth or the Moon, the protection system is ineffective and the instrument high voltages will be turned off.

Table 1
IMAGE WIC Requirement Summary

	Wave-length (nm)	FOV (°)	Pixel size apogee (km)	Angular resolution (°)	Photon collection efficiency (exposure time) (Rayleigh^{-1} pix^{-1} cm^{-2})	Min. Aperture for 1 count pix^{-1} for 100 R source strength (cm^2)
LBH Auroral morphology	140-190	>10	100	0.13	4.1 [10 s]	0.0024
Dayglow	LBH	>10	200	0.26	16 [10 s]	0.0006

The FUV requirements applying to WIC are summarized in Table 1. The first column presents the scientific objective, the second column shows the relevant wavelength region. The field of view (FOV) is derived from the global coverage requirement of the aurora near apogee. The science objective defines the ground resolution, which translates into an angular resolution listed in column 5. As was discussed earlier, the angular resolution defines the photon collection efficiency of the imager in photons Rayleigh^{-1} pix^{-1} cm^{-2} s^{-1}. The FUV images are taken on a rotating spacecraft and the rotation rate is 3 degrees per second (one revolution in every two minutes). The field of view was chosen to be 30° for the WIC in the direction of rotation. Each auroral feature, therefore, spends 10 seconds in the WIC field of view. This consideration defines the exposure time. In the table column representing photon collection efficiency we have included the exposure time and provided the data for the photon collection efficiency for one exposure during one rotation of the spacecraft. The last column is the equivalent aperture required for the instrument to provide the equivalent signal-to-noise ratio for one significant photoelectron count per pixel for a 100 Rayleigh auroral source. These apertures look rather small but we have to realize that they are equivalent apertures and include the actual collecting aperture of the instrument multiplied by the combination of optical transmissions and the applicable efficiencies of conversion of photons into measurable electric charge units. The combined efficiencies for ultraviolet instruments are usually no more than 1 to 2%.

In addition, the various contaminant emissions contribute significantly to the minimum detectable signal. Thus, one count per pixel may be sufficient to produce an acceptable image in the absence of any background, but not in the presence of a background. In summary, we have demonstrated that we needed to optimize the instrument photon collection efficiency while making every effort to minimize the background.

2. Instrument Description

The Earth subtends about 15 degrees when viewed from apogee. In order to image the global aurora it was decided that a full Earth view from apogee would be most advantageous because that would allow full auroral oval coverage even when the satellite is at about one half of the full apogee geocentric distance. The WIC camera attempts to use the available auroral signal in the FUV wavelength band with the exception of OI 130.4 nm emission. A CsI photocathode was used to minimize contamination from the wavelength region longer than 190 nm. To reject UV from wavelengths shorter than 140 nm, we used a 2 mm thick BaF_2 window with an appropriate heater and temperature monitoring system on the window flange. BaF_2 is known to leak in the shorter wavelength region when cold. The refractive index of transparent salts such as MgF_2 vary greatly, and to avoid chromatic aberrations in the wavelength region from 140-190 nm, a reflective system is the best choice. One of the most recent spaceflight FUV cameras, the UVI on the ISTP POLAR satellite, used a three mirror reflective system (Torr, et al., 1995). The resources on IMAGE were more constrained, and since the three mirror system is relatively bulky, we have chosen a concentric two mirror camera of the Viking-Freja type. Some of the IMAGE FUV team members were part of the prior Viking-Freja programs and they were able to offer considerable help and knowledge regarding these cameras. In fact, the front optics graphite fibre epoxy composite (GFEC) tube of the IMAGE WIC flight unit is a Freja flight spare. The type of system is colloquially known as an inverted Cassegrain because the primary is a small convex mirror located in such a manner that the incoming light passes through a hole in the center of a larger, concave secondary (Figure 1). It is a concentric design and both primary and secondary mirrors are spherical and have a common center of curvature. This system is very fast (f/1) and very compact. It has a very serious disadvantage, however, in that it produces the image on a spherical surface and requires that the photocathode be on a spherical surface.

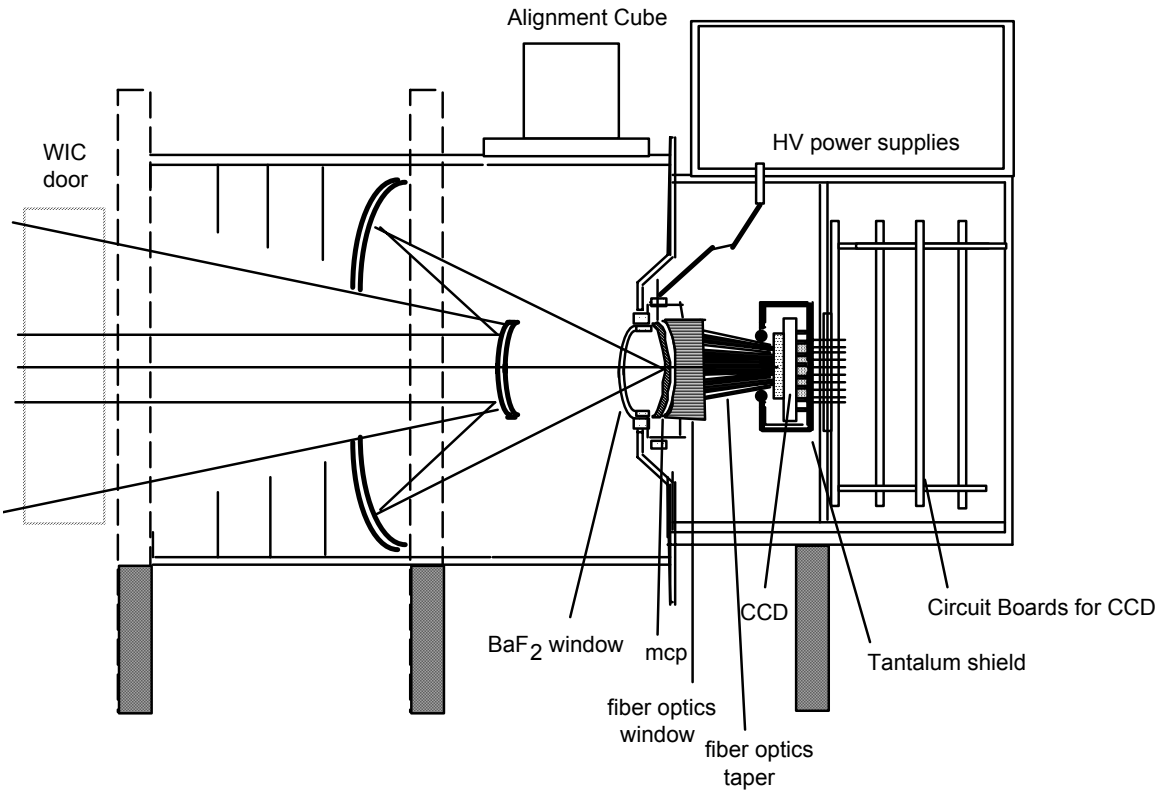

Figure 1. ***Cross sectional schematic of the WIC.***

We considered copying the entire Viking/Freja system to minimize the design risk. The Viking/Freja cameras were also on a rotating spacecraft and operated in the TDI mode. However, the image in the Viking system CCD was not read out in the conventional, fast framing manner. The charge image was integrated on the CCD, and during the integration the charge image was clocked to move in such a way as to compensate for the spacecraft rotation. In order to do this successfully it was necessary to correct the image distortion of the system before imaging on the CCD. In the Viking design this was accomplished by a special fiber optics coupling system that was specially polished and mated to another fiberoptic element. The net result was the removal of the optical distortions. On the advice of the team members who were associated with the Viking design, it was decided that we would not attempt to do this difficult task again. Rather, we would operate IMAGE WIC by digitally removing the distortion.

In the IMAGE WIC design (Figure 1), the camera head operates in a fast frame transfer mode with the CCD being read at approximately 30 full frames (512 by 256 pixel) per second with an exposure time of approximately 33 ms. The image motion is negligible during such a short exposure. Each image is electronically distortion corrected using the look up table scheme, an offset added to each memory address which is proportional to the image shift due to satellite rotation, and the charge signal is digitally summed in memory. The advantage of the electronic distortion correction is that it is extremely flexible, permitting various kinds of corrections, including x and y motions and image rotation.

One of the disadvantages of this approach is that during each spin-scan of the Earth the CCD will be read many (300) times and the resulting CCD read out noise will be added up in the integrated image, and the resultant r.m.s. noise will be larger by the square root of 300 = 17. To minimize this deficiency, the WIC intensifier had to have 17 times more gain to minimize the relative contribution of the CCD read out noise. The digitization of the WIC camera electronics was adjusted so that the peak to peak fluctuation for a single frame readout was just about 3 A-D units. Thus, for a 300 exposure integration, the peak to peak fluctuation was 50 A-D units. The image intensifier gain had to be sufficient to amplify each single photoelectron to the order of 50 A-D units to assure that, on average, a single electron incidence was competitive with the CCD read out noise.

The WIC imager is shown in Figure 2. When this photo was taken the instrument was set up with attached ground support equipment (GSE), including an ion pump to keep the image intensifier chamber under vacuum. This set up permitted the testing of the instrument in air, the application of high voltages, and the illumination of the photocathode with ultraviolet light. For flight, however, the pipes and the attached stainless steel bellows will be

removed and replaced with a purge fitting. This purge fitting allows communication between the detector and instrument cavities. The instrument will be purged with dry nitrogen during all phases of integration up to launch. The instrument has a front cover door not shown in Figure 2. This door will be closed during normal purging and will be opened on orbit, where the detector will be evacuated through the optical cavity.

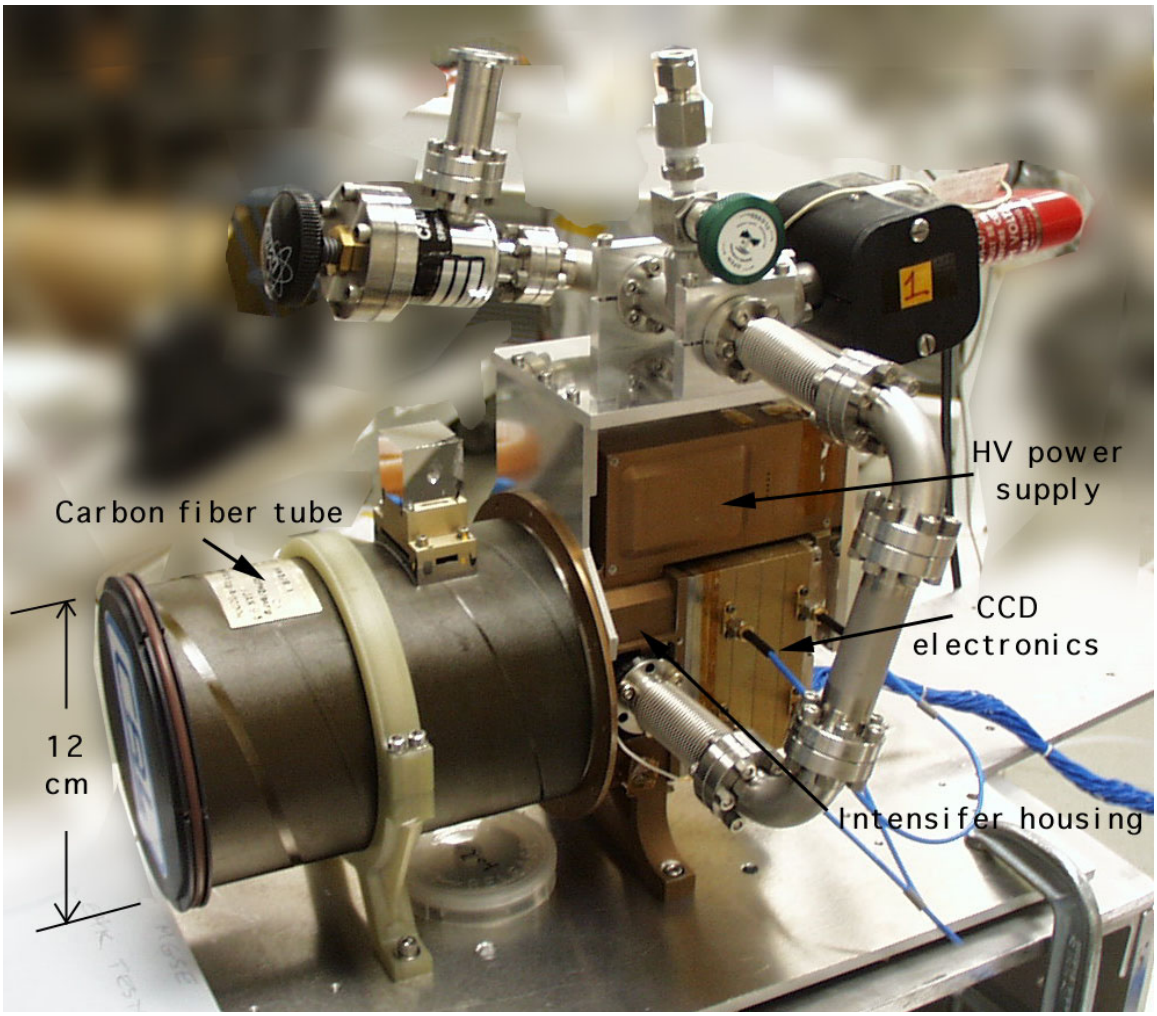

Figure 2. Photograph of the WIC camera flight unit. The stainless steel plumbing and the bare aluminum support structure are GSE. The black ion pump is also GSE. The round tube is the carbon fiber optical tube holding baffles and the primary and secondary mirrors. The alignment cube is mounted on top of the tube. Besides the carbon fiber tube body, the camera consists of alodyne coated units: top is the high voltage power supply, bottom left image intensifier housing, and bottom right the CCD electronics.

The WIC instrument is shown schematically in Figure 1. Light enters from the left and is reflected by the small primary mirror. The secondary mirror reflects the light towards the photocathode around the periphery of the primary mirror. There is a curved BaF_2 entrance window on the detector to reject radiation short of 140 nm in wavelength. Inside the detector, a curved microchannel plate is mounted and the cesium iodide photocathode is evaporated on the concave side. A photoelectron, which is emitted by the photocathode, is accelerated down into the MCP pores and will multiply through secondary emission by colliding with the walls. It has been customary to place a mesh in front of the photocathode and to apply a negative potential to the mesh. The purpose of such a mesh was to supply an additional electric field in front of the MCP to accelerate the electrons into the MCP pores, and at the same time to discourage the lateral spread of electrons on the input side. Such meshes have been shown to increase the effective quantum efficiency of MCPs. This technique was not adopted for the WIC because it was thought that any added electrode with high negative potential would contribute additional photo emissions excited

by out of band UV and visible radiation. The minimization of those emissions was considered to be of greater importance than improvement of a few percent in effective quantum efficiency. It should be noted that the application of an FUV photocathode to a surface actually reduces the near UV response when compared to bare, untreated metal such as a mesh.

At the back end of the MCP, the electron avalanche is accelerated towards the phosphor by an electric field applied between the back end of the MCP (ground) and the phosphor (+4000V), which is deposited on the concave side of the fiberoptic output window. The phosphor is coated with aluminum on the MCP side to minimize light from returning toward the MCP and to prevent light from the optics from directly reaching the CCD.

There are two high voltage supplies with remotely programmable outputs mounted on the WIC camera. One of them supplies the input end of the microchannel plate with negative voltages and provides a commandable accelerating voltage level between 900 and 1200 volts. The MCP gain depends on this voltage. The other power supply provides positive 4000 volts to the phosphor. On the back of the detector, the fiberoptic window is flat and a tapered fiberoptic plug is bonded to it. The plug transfers the image to the CCD with a demagnification of 1.75 to 1. Of the 512 x 512 pixels (pixel spacing of 15 μm), only 512 x 256 pixels of the CCD are active. The 512 direction is in the plane of rotation.

CCDs are known to be sensitive to proton bombardment because protons generate traps in the silicon that impair the charge transfer efficiency. To assure that the CCD will survive the proton exposure of the IMAGE spacecraft orbit, a proprietary, radiation-tolerant CCD, developed for the Lockheed-Martin star tracker systems was used, and a tantalum shielding cup (of 4 mm thickness weighing 450 g) was installed to surround the CCD. To minimize mechanical loading on the CCD, it is bonded to the fiberoptic taper and connection is made to the circuit board through pushpins, which minimize the force on the CCD assembly. There are several circuit boards in the front-end camera. Some of them are digital, supplying the clock wave forms for the CCD to accomplish frame transfers and subsequent read out on a line-by-line and on a pixel-by-pixel basis. Another board processes the video from the CCD using a delay line based, fast double-correlated sampler design. The camera outputs the information digitally in the form of A-D converted 8-bit bytes, one per pixel.

As was discussed before, the WIC optics was originally built as a spare for the Canadian Freja program. The housings were disassembled and the mirrors were taken out. New mirrors were fabricated to the old specifications under the supervision of Canadian Astronautics Limited (CAL), who was the original contractor for the Viking/Freja cameras. The new mirrors were coated by special multi-layer coating, which had low reflectivity in the visible and near UV region. The coatings were made using the technology developed for the ISTP/POLAR UVI imager filters (Torr et al., 1995). In parallel, sample coatings were deposited on flat substrates to evaluate them at all angles used in the WIC design. Their normal angle of incidence reflectivity is presented as Figure 3. The large fluctuations in the reflectivity are real because the measurement accuracy is better than a few percent. Note that having the two mirrors in the WIC means that the resultant reflectivity is the product of the two reflectivities. This mirror coating provides additional visible and near UV suppression.

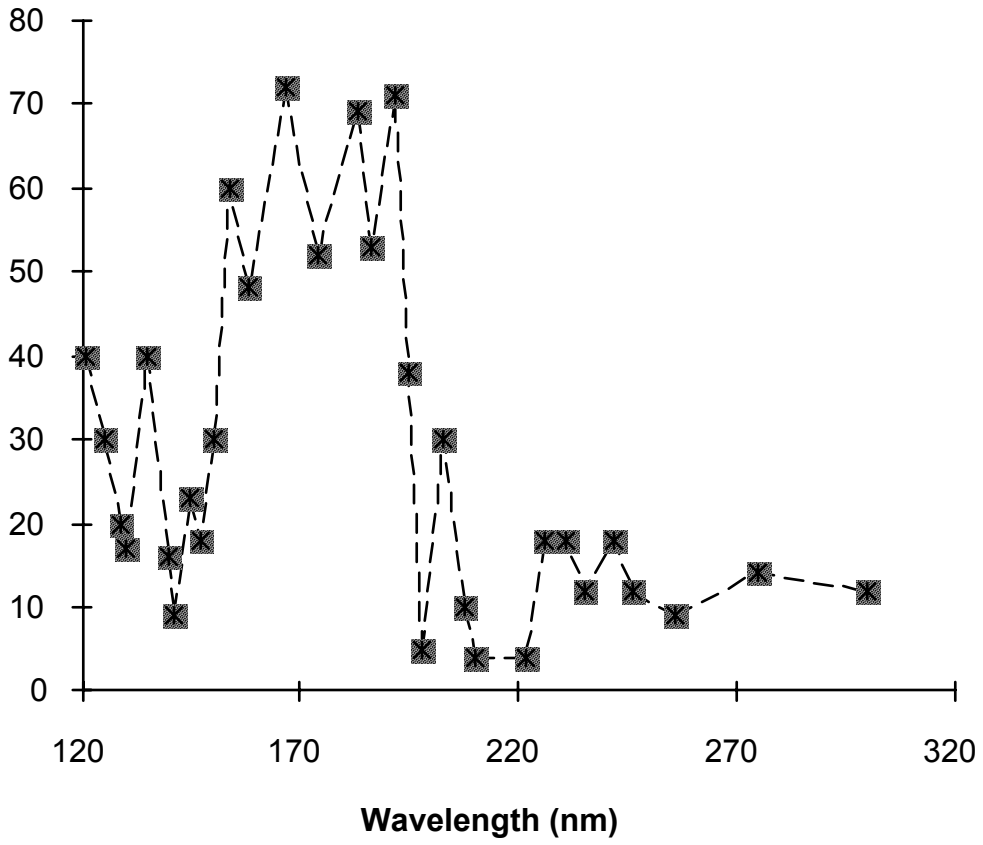

Figure 3. *Coating on the WIC mirrors.*

Originally we considered purchasing sealed image intensifiers from the same source used by Freja. Unfortunately, the past supplier of the tubes declined our order because they could no longer obtain the needed curved MCPs. Fortunately, we had the expertise to make detectors for the far UV spectral range at the University of California Berkeley (UCB). The detectors custom built at UCB were not sealed tubes and, therefore, needed to be connected to a vacuum system while in operation. The vacuum of space will evacuate them in orbit. In order to maximize cleanliness and to allow ground testing of the instrument (outside of a vacuum chamber) the detectors were made vacuum tight so that an attached ion pump could be operated to evacuate the detectors (Figure 2). This approach was used extensively during final testing and spacecraft integration.

The curved MCPs were produced by Photonis in France. The method of manufacture consisted of slicing a glass boule into wafers, and then grinding the flat surfaces of the wafers to the appropriate curvature. The pore fill was then dissolved and the resultant MCP was baked in a hydrogen atmosphere to create the semi-conducting film on the surface of the glass. This technique yielded a MCP with a constant bias angle with respect to the optic axis. Since the MCP was curved and the bias angle was constant, the pore length varied depending on the position on the MCP producing large gain non-uniformities. This was found to be a serious disadvantage because peak to peak variations of ≈30% were observable over the MCP surface and WIC would not have been acceptable as a staring imager without the TDI averaging process. Because of the serious schedule pressure of the short-duration IMAGE program, it was decided to orient the MCP in such a way that the non-uniformities were minimized in the direction perpendicular to the direction of TDI scanning. This way the TDI-ed net result will be a great deal more uniform than an individual WIC frame. The downside of this deficiency is that it resulted in a small region of extremely low gain MCP on the extreme right side of the CCD. This region will be suppressed by using the look up tables so that the CCD read out noise contribution from this area will also be excluded.

The Lockheed-Martin Palo Alto Research Laboratories built the CCD and the associated electronics. As mentioned previously, the WIC camera operated in a photon counting mode. In this mode the gain was sufficiently high (MCP voltage of >1050 V) that each photoelectron produced a detectable individual bright scintillation in a single frame CCD image. The output of the CCD is an 8 bit number representing the digitized value of the charge collected in a specific pixel during the previous 30 ms single frame integration. In a single test exposure, the A-D units contained by each spot were summed and the results were compiled in a histogram shown in Figure 4. It can be seen that the mean size of a photoelectron scintillation spot is of the order of 100 CCD A-D units at this MCP voltage. During WIC on orbit operation the exposure will be the result of the integration of about 300 frames. The frames are digitally added into a 16 bit TDI memory. The histogram produced in Figure 4 can be repeated on orbit and the high voltage adjusted to compensate for potential gain changes.

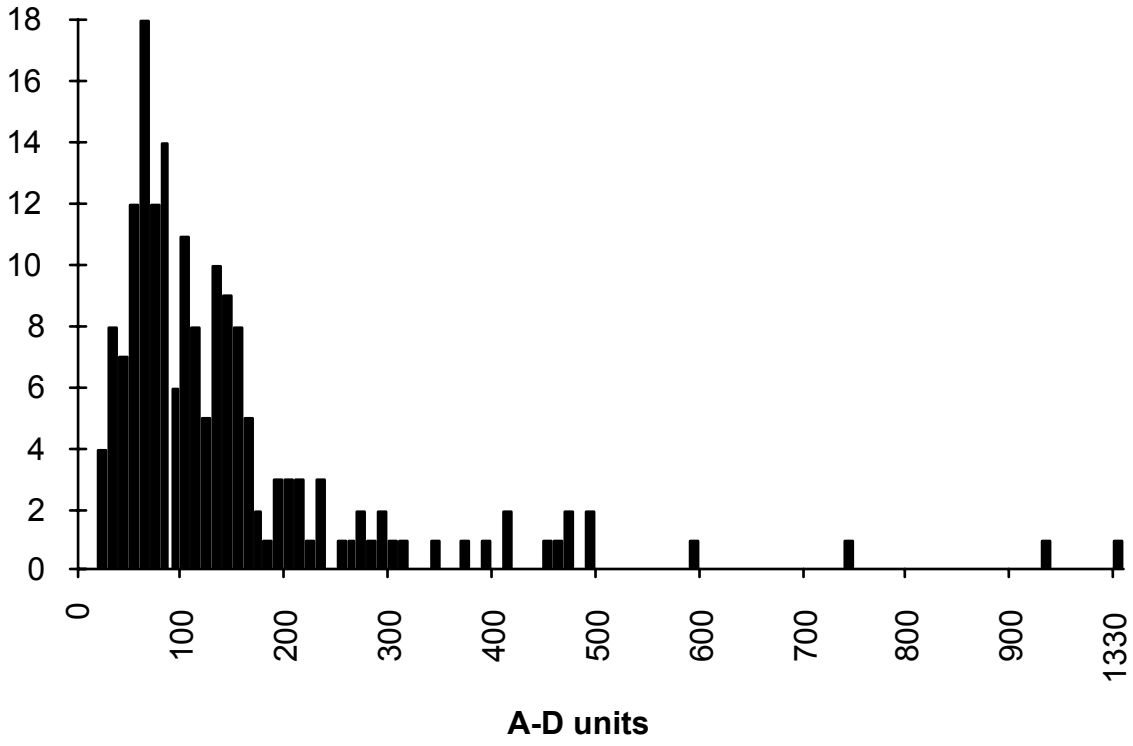

Figure 4. WIC pulse height distribution in CCD digitization units.

The measurement of the average size of the scintillation allows estimation of the overall quantum efficiency of the WIC detector system. During the calibration process, the signal output in CCD A-D units was measured as a function of photon flux incident on the primary optics. When this number was converted into the number of average size scintillations, it was possible to obtain the number of detected photons as a function of the input photon flux (photons cm^{-2}). This ratio provides the WIC effective aperture. This result is plotted as a function of wavelength in Figure 5. The overall response is a combination of the relatively smooth photocathode response and the undulating reflectivity of the mirrors shown in Figure 3. The instrument resources have been tabulated in Table 2.

Table 2
WIC resource utilization

Mass (kg)	Volume (cm^3)	Power Standby (W)	Power Acquire (W)
4.1	327 x 175 x 180	.84	3.90

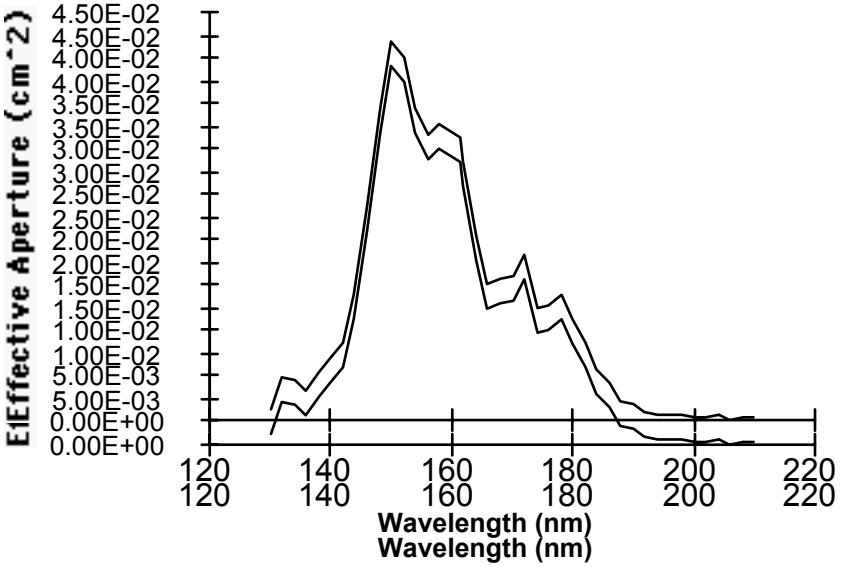

Figure 5. WIC effective aperture as a function of wavelength.

3. Instrument Calibrations

After the WIC camera was completed it underwent a thorough testing and evaluation program. The instrument, with its appropriate GSE, was moved to the Marshall Spaceflight Center in Huntsville, Alabama. There it was installed into a calibration tank that had the facility of producing monochromatic ultraviolet beams of selectable wavelength. It was important to have a uniform and parallel beam. This was accomplished by introducing a thin slab of sand blasted MgF_2 near the output of the monochromator near the focus of the collimator. The resultant beam profile was 60 mm in diameter and uniform within 30%. The pixel resolution measured as a function of MCP voltage is presented in Figure 6. The solid curve is FWHM in the x direction, and the dotted curve is resolution in the y direction. The third, steeply rising curve represents the total number of counts (CCD A-D units) in thousands within the resolution spot. As the voltage is increased, a slight increase in the spot size is accompanied by a large increase in overall gain. Note that a CCD pixel is 26 μm at the intensifier. Thus, the resolution spot size of the optics and image intensifier combination is about 2 pixels.

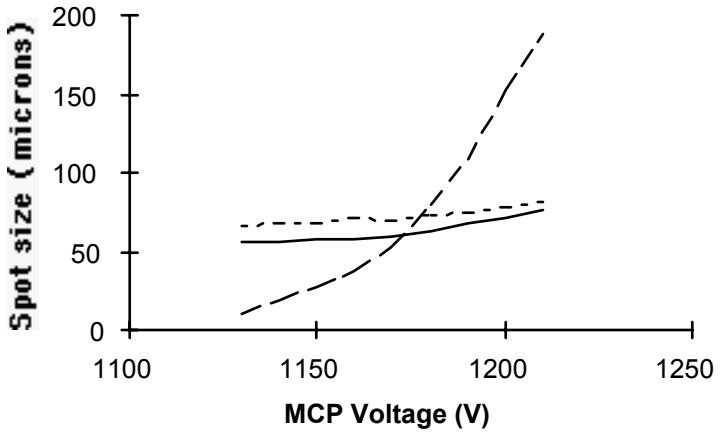

Figure 6. *WIC spot size in microns. Solid line in x direction, short dashed line in y direction. Spot size increases slightly with MCP gain. Dashed line with long dashes represents the total spot intensity in 1000 CCD A-D units.*

The instrument resolution was also calibrated as a function of temperature and it was found that the instrument focus was extremely temperature sensitive. The operating temperature range of the instrument was from -20^o C to +40^o C. The instrument was focused at 23^o C and the defocusing was particularly pronounced when the instrument was operated at the lower temperature range of -20^o C. Even at 0^o C the resolution spot developed three sub-spots corresponding to the three regions of the pupil as divided by the spider holding the primary mirror. At -20^o C the spots grew so large that their intensity diminished considerably and they were hardly perceptible. This deficiency was observed quite late in the WIC development and an extensive search for the cause was undertaken. It was proven that the problem was with the mounting of the optical system, and to minimize the problem a heater was added on the last baffle located near the back side of the secondary mirror. A thermistor was also bonded on the back of the secondary mirror. This heater and its thermistor were able to control the temperature of the optical mounting elements near the secondary mirror. It was shown that with the heater operating, the instrument remained in focus when subjected to -20^o C environment.

It was discussed in Paper 1 that the FUV system, the SI and the WIC, had to operate on a rotating platform in the so called TDI mode, and that to preserve the resolution, the imager distortions had to be corrected on orbit in real time. It was, therefore, important to obtain calibration data to determine appropriate input coefficients for the distortion correction look up tables. This data was obtained by turning the instrument through various angles around axes located near the entrance aperture while observing the spot corresponding to a collimated beam in the image. The angles and the corresponding x and y pixel locations were recorded to provide a matrix to find coefficients for least square fitting used in the distortion correction look up tables. The pixel responses for such a matrix were plotted in Figure 7. Figure 7 shows the degree of distortion in the WIC camera that has to be removed by the look up table.

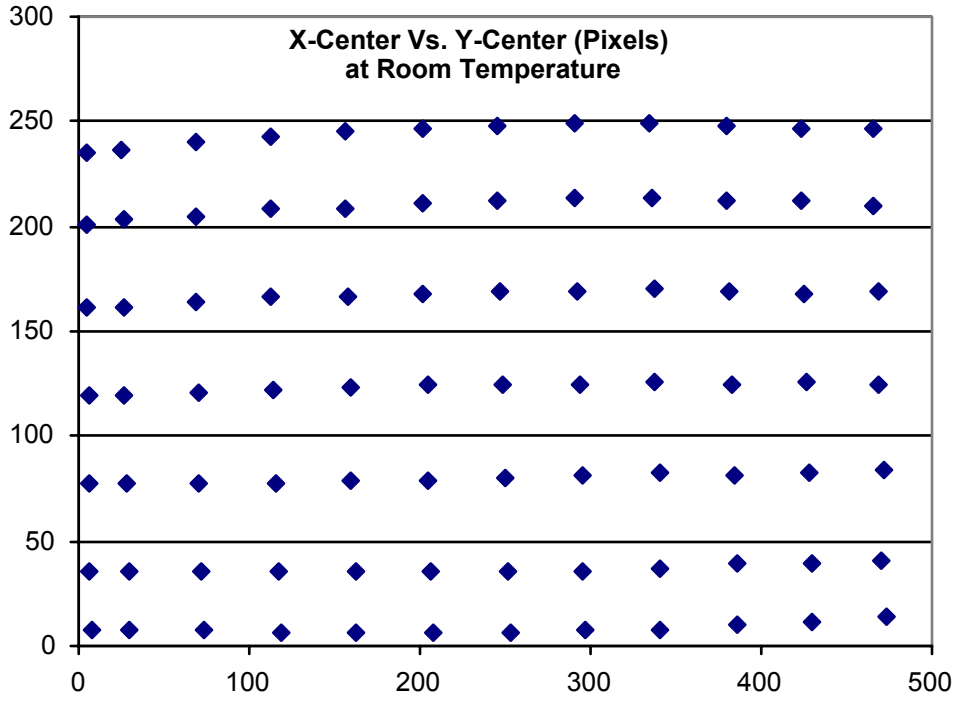

Figure 7. *Pixel values corresponding to the input angles of the collimated beam.*

From the data in Figure 5 it can be seen that the equivalent aperture at peak response is about 0.04 cm^2. The WIC resolution element field of view (resolution cell size) is approximately double the pixel size i.e. 0.18°. Using this as the angular size of a resolution cell, it provides a photon collection efficiency of 5.7 photons cm^{-2} R^{-1} $cell^{-1}$ for the exposure duration of about 10 s. Thus, a 100 Rayleigh UV aurora would produce a signal to noise ratio consistent with 23 equivalent photoelectrons per pixel at the peak of the instrument response. The spectral response match of the WIC compared with a model LBH auroral spectrum is shown in Figure 8.

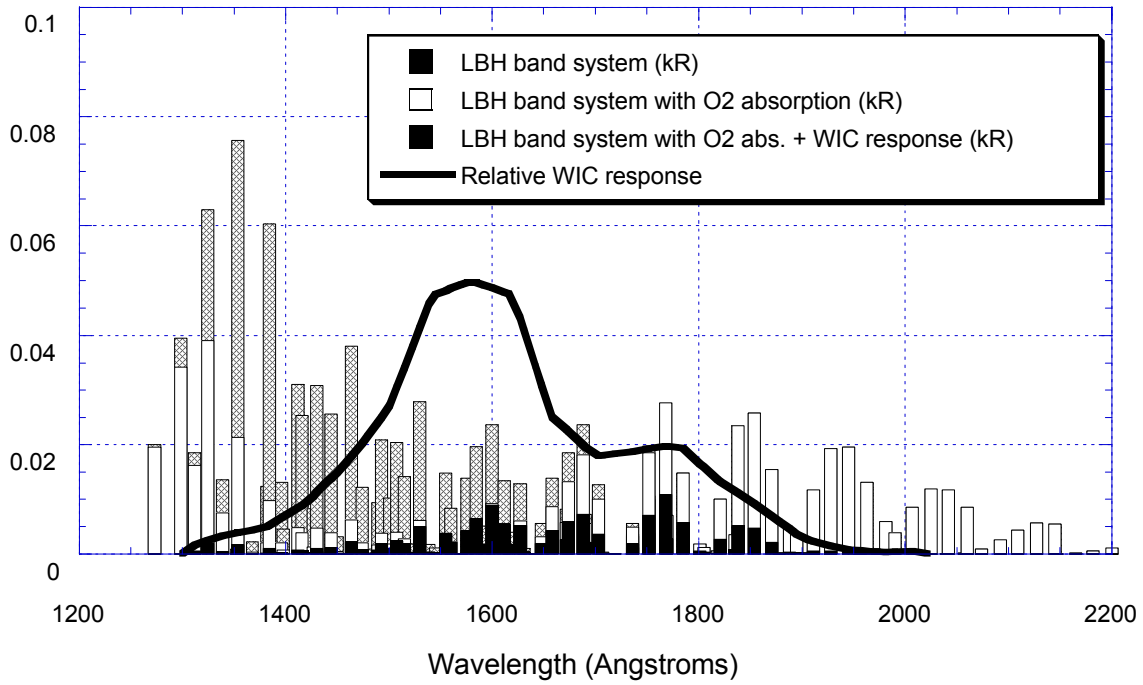

Figure 8. WIC response superimposed on a model of the LBH bands in the far UV wavelength range produced by 10 keV electrons.

Table 3
IMAGE WIC Instrument Performance Summary

Pixel Size (^{o})	Res. cell size (^{o})	Res. cell at apog. (km)	Res. cell at perig. (km)	Photon Collection cm^{-2} R^{-1} $cell^{-1}$	Meas. equiv. aperture A_e (cm^2)	Counts $cell^{-1}$ / 100 R/exposure
0.09	0.18	120	3.1	5.7	0.04	23

The instrument parameters are summarized in Table 3. The first column is the pixel size, the angular area associated with one memory element. The second column is the resolution cell size, which is the resolution full width at half maximum of the measured point spread function. On the WIC this quantity is approximately twice the pixel diameter. Column 3 and 4 represent the size of the resolution cell projected to the Earth from apogee and perigee, respectively. The resolution cell size defines the solid angle from which photons are collected and allows us the calculation of the photon collection efficiency per square cm during the exposure time. This is presented in column 5. Column 6 is the equivalent aperture A_e of each system as discussed earlier. This, combined with the photon collection efficiency, provides the number of significant quanta (column 7) per 100 Rayleigh source within the resolution cell of the instrument for a single spin of the spacecraft. Column 6, A_e, can be compared directly to the values in Table 1 expressing the instruments scientific requirements.

In summary, we have shown that WIC satisfies the IMAGE requirements. It has adequate resolution and sensitivity. There are, however, some lessons we have learned from developing the WIC instruments. The deeply curved photocathode was a source of many problems. One of these problems was the serious gain variation across the MCP. This defect was attributed to the MCP pore bias angle variation across the image. In general, it seems that the detectors are the most difficult parts of this type of imager. Therefore, it would be worthwhile to use systems that produce flat image planes at the expense of some optical complexity to allow the use of a simpler, flat detector.

References

Anger, C. D., S. K. Babey, A. L. Broadfoot, R. G. Brown, L. L. Cogger, R. Gattinger, J. W. Haslett, R. A. King, D. J. McEwen, J. S. Murphree, E. H. Richardson, B. R. Sandel, K. Smith and A. Vallance Jones, An ultraviolet auroral imager for the Viking spacecraft, *Geophys. Res. Lett.,* 14, 387-390, 1987.

Burch, C. R., Reflecting microscopes, *Proc. Phys. Soc.,* 59, 41, 1947.

Cogger, L. L., D. J. Hearn, J. S. Murphree, R. A. King, E. P. King, Y. I. Galperin, B. Gordon and J. Matsushita, Ultraviolet Auroral Imager (UVAI), in Interball Mission and Payload, edited by Y. Galperin, T. Muliarchik and J. P. Thouvenin, Russian Space Agency, Space Research Institute and French Space Agency, 382, 1995.

Frank, L. A., J. D. Craven, K. L. Ackerson, M. R. English, R. H. Eather and R. L. Crovillano, Global auroral imaging instrumentation for the Dynamics Explorer mission, *Space Sci. Instrum.,* 5, 369-393, 1981.

Murphree, J. S., R. A. King, T. Payne, K. Smith, D. Reid, J. Adema, B. Gordon and R. Wlochowicz, The Freja Ultraviolet Imager, *Space Science Reviews,* 70, 421-446, 1994.

Torr, M.R., D. G. Torr, M. Zukic, R.B. Johnson, J. Ajello, P. Banks, K. Clark, K. Cole, C.Keffer, G. Parks, B. Tsuratani, and J. Spann, A far ultraviolet imager for the International Solar-Terrestrial Physics mission., *Space Science Reviews*, 71, 329, 1995.